AERO 660: Final Project

Exploring Delayed Feedback in the van Der Pol Oscillator using Perturbation Methods

Lesley A. Weitz

07 December 2007

Abstract

This project examines the behavior of the van der Pol oscillator with delayed position feedback. Multiple-scales perturbation methods are applied to describe the amplitude and phase of the limit cycle. Results show that the feedback gain and time delay can be used to eliminate the limit-cycle behavior. Numerical simulations are used to confirm analytical results, and further research ideas are discussed.

1 Introduction

Limit cycles are periodic oscillations that arise in nonlinear systems even in the absence of a periodic-forcing input. The standard limit cycle of a nonlinear system can be described by a period, waveform, and amplitude, and any perturbation from a stable limit cycle will return to the standard limit cycle.[1] Limit cycles can occur in different types of dynamical systems including biological systems, airplane-wing flutter, and bridge design. In many of these cases, there is a need to control or modify limit-cycle behavior in order to avoid dangerous periodic behavior. Research seeks to answer the question: how can different feedback-control designs modify the limit-cycle period, waveform, and amplitude?

This project investigates the behavior of the van der Pol oscillator when the control input is a feedback of the position delayed by some time, τ. In the actual implementation of feedback control, delays in the state feedback can occur due to inherent measurement and sensing delays. These delays may need to be taken into account when evaluating closed-loop system behavior. Therefore, the importance of understanding delay effects on a system can be clearly seen. This project shows that delays in the position feedback to the van der Pol oscillator can be exploited to eliminate limit-cycle oscillations.

Multiple-scale perturbation techniques can be used to approximate the behavior of the weakly-damped oscillator with delayed position feedback, and this approach will be used to derive ordinary differential equations that describe the amplitude and phase of the limit cycle. The organization of the project is as follows: Section 2 will present the van der Pol oscillator equations, Section 3 discusses the two perturbation techniques used to investigate the delayed equation, nonlinear analysis of the amplitude and phase equations is presented

in Section 4, and conclusions are presented in Section 5.

2 Van der Pol Oscillator with Delay

The van der Pol Oscillator, shown below, is a classical example of a nonlinear dynamical system that displays limit cycle oscillations. Therefore, this model serves as a prototypical example in which to investigate control design to avoid dangerous limit-cycle behavior.

$$\ddot{x} + \epsilon(x^2 - 1)\dot{x} + x = f(t), \quad \epsilon > 0 \tag{1}$$

When the forcing input, $f(t)$, is zero, there is a stable limit cycle that attracts all solutions starting at $(x(0), \dot{x}(0))$ except at the origin.[1,2] For the *strongly nonlinear damping* case or $\epsilon >> 1$, the limit cycle displays two widely separated time scales. One time scale is related to a slow buildup and the second scale is related to a sudden discharge. In the *weakly nonlinear damping* case or $\epsilon << 1$, the limit-cycle behavior may closely approximate a simple harmonic oscillator, $\ddot{x} + x = 0$, for a short time.

Challenges in understanding the behavior of the van der Pol oscillator are encountered when the forcing function in equation (1) is nonzero. In the *weakly nonlinear damping* case, perturbation methods can be used to approximate a solution to the forced equation. Several researchers have investigated the approximation of weakly-damped nonlinear equations with delayed feedback,[2–4] and this project will investigate the van der Pol oscillator with feedback of the form $f(t) = \epsilon k x(t - \tau)$. The forced van der Pol equation is shown below.

$$\ddot{x} + x = \epsilon \left[(1 - x^2)\dot{x} + kx(t - \tau)\right] \tag{2}$$

Equation (2) is a delay-differential equation (DDE) due to the delayed-state term, $x(t - \tau)$.

DDEs pose several challenges in stability analysis and control design due to an infinite number of solutions that can satisfy the DDE;[5,6] however, these issues will not be discussed further here. This project uses two separate multiple-time-scales perturbation approaches in order to approximate the behavior of the above DDE.

3 Multiple Time-Scales Approach

Regular perturbation theory, where solutions are approximated as $x(t) = x_0(t) + \epsilon x_1(t) + O(\epsilon^2)$, cannot be applied to weakly nonlinear systems because those systems typically exhibit two time scales: a fast time scale for oscillatory behavior and a slow time scale over which the amplitude decays.[1] A multiple time scales approach rectifies the presence of two distinct time scales in the solution, and for the van Per Pol oscillator, a two-scale method is sufficient to describe the behavior of the oscillator. Both approximation techniques presented here exploit the presence of the fast and slow time scales. The first method uses the method of averaging to derive differential equations that describe the amplitude and phase of the solution to equation (2), and the second method uses a two-scale expansion of the method of multiple scales from which the equations describing the amplitude and phase are similarly derived.

3.1 Method of Averaging

The van der Pol equation with feedback delay in equation (2) can be written as

$$\ddot{x} + x = \epsilon g(x, \dot{x}, x_\tau); \quad g(x, \dot{x}, x_\tau) = (1 - x^2)\dot{x} + kx_\tau, \tag{3}$$

where $x_\tau = x(t-\tau)$. To approximate the solution to the above equation, an amplitude-phase transformation is proposed where the solution to equation (3) is assumed to have the following form.

$$x(t) = r(t)\cos\left(t + \phi(t)\right)$$

$$\dot{x}(t) = -r(t)\sin\left(t + \phi(t)\right)$$

These are the Krylov-Bogoliubov-Mitropolsky (KBM) equations.[7,8] In the case that $\epsilon = 0$, $x(t) = \cos(t+\phi)$, but in the case of small ϵ, r and ϕ become slowly-varying functions of time. The condition $\dot{r}\cos(t+\phi) - r\dot{\phi}\sin(t+\phi) = 0$ leads to the derivative $\dot{x} = -r\sin(t+\phi)$ as shown above.

The KBM equations are substituted into equation (3), from which expressions for $\dot{r}$ and $r\dot{\phi}$ can be easily found.

$$\begin{aligned}
-\dot{r}\sin(t+\phi) - r(1+\dot{\phi})\cos(t+\phi) + r\cos(t+\phi) &= \\
&= \epsilon g(r\cos(t+\phi), -r\sin(t+\phi), r_\tau\cos(t-\tau+\phi_\tau) \\
-\dot{r}\sin(t+\phi) - r\dot{\phi}\cos(t+\phi) &= \epsilon g(\cdot,\cdot,\cdot) \qquad (4)
\end{aligned}$$

$$\dot{r} = -\epsilon\sin(t+\phi)g(\cdot,\cdot,\cdot)$$

$$r\dot{\phi} = -\epsilon\cos(t+\phi)g(\cdot,\cdot,\cdot)$$

Note that $\dot{r}$ and $\dot{\phi}$ are 2π-periodic functions due to the presence of the $\sin(t+\phi)$ and $\cos(t+\phi)$ terms.

In the method of averaging, the right hand sides of the above equations are replaced with their averages over 2π.[1,2] The amplitude and phase variables are treated as constants due

to their slowly-varying nature, and thus, $r_\tau = r(t-\tau)$ and $\phi_\tau = \phi(t-\tau)$ can also be treated as constants. The averaged equations can be written as shown below.

$$\begin{aligned}\dot{r}(t) &= -\epsilon < \sin(t+\phi), \left[1 - r^2\cos^2(t+\phi)\right]\left[-r\sin(t+\phi)\right] + kr\cos(t-\tau+\phi) > \\ &= \epsilon r < \sin^2(t+\phi) > -\epsilon r^3 < \sin^2(t+\phi)\cos^2(t+\phi) > - \\ &\quad - \epsilon kr\cos(\tau) < \sin(t+\phi)\cos(t+\phi) > -\epsilon kr\sin(\tau) < \sin^2(t+\phi) >\end{aligned}$$

The averages over 2π can be evaluated using the definition below.

$$< fg >= \frac{1}{2\pi}\int_0^{2\pi} f(\theta)g(\theta)d\theta \tag{5}$$

Therefore, the averages of the trigonometric functions are easily determined.[1]

$$\begin{aligned}&< \sin\theta\cos\theta >= 0, \quad < \sin^2\theta >=< \cos^2\theta >= \frac{1}{2}, \\ &< \sin^2\theta\cos^2\theta >= \frac{1}{8}, \quad < \cos^3\theta\sin\theta >= 0\end{aligned}$$

Hence, the averaged expression for $\dot{r}$ can be found.

$$\dot{r} = \frac{\epsilon r}{2}\left(1 - \frac{r^2}{4} - k\sin\tau\right) \tag{6}$$

The expression for $r\dot{\phi}$ is found similarly.

$$\begin{aligned}r\dot{\phi}(t) &= -\epsilon < \cos(t+\phi), \left[1 - r^2\cos^2(t+\phi)\right]\left[-r\sin(t+\phi)\right] + kr\cos(t-\tau+\phi) > \\ &= \epsilon r < \cos(t+\phi)\sin(t+\phi) > -\epsilon r^3 < \cos^3(t+\phi)\sin(t+\phi) > - \\ &\quad - \epsilon kr\cos(\tau) < \cos^2(t+\phi) > -\epsilon kr\sin(\tau) < \cos(t+\phi)\sin(t+\phi) > \\ &= -\frac{\epsilon r}{2}k\cos\tau\end{aligned}$$

Thus, equations describing the evolution of the amplitude and phase can be derived by averaging the delay-differential equations over 2π. These results are presented again below

in their final form.

$$\dot{r} = -\frac{\epsilon r}{2}\left(\frac{r^2}{4} - 1 + k\sin\tau\right) \tag{7}$$

$$r\dot{\phi} = -\frac{\epsilon r}{2}k\cos\tau \tag{8}$$

3.2 Method of Two-Timing

The method of two-timing is an alternate approach to derive the differential equations that describe the amplitude and phase equations. Here, a solution of the form below is assumed.

$$x(t) = x_0(T_0, T_1) + \epsilon x_1(T_0, T_1) + O(\epsilon^2) \tag{9}$$

The time scale $T_0 = t$ is the fast time scale, and $T_1 = \epsilon t$ is the slow time scale. First and second derivatives with respect to time t can be written using differential operators.

$$\frac{d}{dt} = \frac{\partial}{\partial T_0} + \epsilon\frac{\partial}{\partial T_1} + 0(\epsilon^2) \equiv D_0 + \epsilon D_1 + 0(\epsilon^2)$$
$$\frac{d^2}{dt^2} = \frac{\partial^2}{\partial T_0^2} + 2\epsilon\frac{\partial}{\partial T_0 \partial T_1} + 0(\epsilon^2) \equiv D_0^2 + 2\epsilon D_0 D_1 + O(\epsilon^2)$$

Therefore, $\dot{x}(t)$ and $\ddot{x}(t)$ can be expressed using differential operators.

$$\begin{aligned}\dot{x}(t) &= (D_0 + \epsilon D_1)\left[x_0(T_0, T_1) + \epsilon x_1(T_0, T_1) + O(\epsilon^2)\right] \\ &= D_0 x_0(T_0, T_1) + \epsilon\left[D_0 x_1(T_0, T_1) + D_1 x_0(T_0, T_1)\right] + O(\epsilon^2)\end{aligned} \tag{10}$$

$$\begin{aligned}\ddot{x}(t) &= (D_0^2 + 2\epsilon D_0 D_1)\left[x_0(T_0, T_1) + \epsilon x_1(T_0, T_1) + O(\epsilon^2)\right] \\ &= D_0^2 x_0(T_0, T_1) + \epsilon D_0^2 x_1(T_0, T_1) + 2\epsilon D_0 D_1 x_0(T_0, T_1) + O(\epsilon^2)\end{aligned} \tag{11}$$

Equations (10) and (11) can then be substituted into equation (2) with $x(t-\tau) = x(T_0 - \tau, T_1) = x_{0_\tau} + \epsilon x_{1_\tau} + O(\epsilon^2)$ where it is assumed that the effect of the delay on the slow time

scale can be neglected.

$$\begin{aligned} D_0^2 x_0 + \epsilon D_0^2 x_1 + 2\epsilon D_0 D_1 x_0 + x_0 + \epsilon x_1 = \\ = \epsilon \left[1 - x_0^2 - 2\epsilon x_0 x_1 + O(\epsilon^2)\right] \left[D_0 x_0 + \epsilon(D_0 x_1 + D_1 x_0) + O(\epsilon^2)\right] + \\ + \epsilon k \left[x_{0_\tau} + \epsilon x_{1_\tau} + O(\epsilon^2)\right] \end{aligned} \tag{12}$$

Gathering the $O(1)$ and $O(\epsilon)$ terms yields two differential equations, respectively.

$$D_0^2 x_0 + x_0 = 0 \tag{13}$$

$$D_0^2 x_1 + x_1 = -2D_0 D_1 x_0 + D_0 x_0 - x_0^2 D_0 x_0 + k x_{0_\tau} \tag{14}$$

Equation (13) is a simple, harmonic oscillator with a solution given by $x_0(T_0, T_1) = a(T_1)\cos T_0 + b(T_1)\sin T_0$. This solution can also be written using a complex form.

$$\begin{aligned} x_0(T_0, T_1) &= A(T_1)e^{iT_0} + \bar{A}(T_1)e^{-iT_0} \\ &= A(T_1)e^{iT_0} + cc \end{aligned} \tag{15}$$

The cc term refers to the complex conjugate term, which will be used where appropriate. Additionally, $A(T_1)$ can be expressed in a polar form with an amplitude $\alpha(T_1)$ and phase $\beta(T_1)$.[4,7]

$$A(T_1) = \frac{1}{2}\alpha(T_1)e^{i\beta(T_1)} \tag{16}$$

The $x_0(T_0, T_1)$ solution and its appropriate derivatives can be substituted into equation (14); the derivatives of $x_0(T_0, T_1)$ on the right-hand side of equation (14) are detailed in the Appendix. The resulting substitution is given below with references to T_0 and T_1 dropped for notational purposes.

$$D_0^2 x_1 + x_1 = -i2A'e^{iT_0} + iAe^{iT_0} - iA^3 e^{i3T_0} - iA^2\bar{A}e^{iT_0} + kAe^{i\tau}e^{iT_0} + cc \tag{17}$$

The objective is to find a solution to x_1 that is free of secular terms, i.e., the coefficients of the resonant terms should be set to zero. Therefore, the sum of the e^{iT_0} terms should equal zero.

$$(-i2A' + iA - iA^2\bar{A} + kAe^{i\tau})e^{iT_0} = 0 \tag{18}$$

Substituting the polar form of $A(T_1)$ into equation (18) and separating the real and imaginary parts yields the following equations, respectively.

$$\alpha' \sin\beta + \alpha\beta' \cos\beta - \frac{1}{2}\alpha \sin\beta + \frac{1}{8}\alpha^3 \sin\beta + \frac{1}{2}k\alpha(\cos\beta\cos\tau + \sin\beta\sin\tau) = 0 \tag{19}$$

$$-\alpha' \cos\beta + \alpha\beta' \sin\beta + \frac{1}{2}\alpha \cos\beta - \frac{1}{8}\alpha^3 \cos\beta + \frac{1}{2}k\alpha(\sin\beta\cos\tau - \cos\beta\sin\tau) = 0 \tag{20}$$

Both equations (19) and (20) are function of α' and β'. Multiplying equation (19) by $\sin\beta$ and equation (20) by $\cos\beta$ and subtracting the second equation from the first isolates the α' term.

$$\alpha' - \frac{1}{2}\alpha + \frac{1}{8}\alpha^3 + \frac{1}{2}k\alpha \sin\tau = 0 \tag{21}$$

Similarly, multiplying equation (19) by $\cos\beta$ and equation (20) by $\sin\beta$ and adding the two equations isolates the β' term.

$$\alpha\beta' + \frac{1}{2}k\alpha \cos\tau = 0 \tag{22}$$

By replacing α with r and β with ϕ and evaluating the derivative with respect to $T_0 = t$ rather than with respect to $T_1 = \epsilon t$, it can be seen that the amplitude and phase equations derived using the two-timing method are the same as those derived using the averaging method.

$$\frac{\dot{r}}{\epsilon} = \frac{1}{\epsilon}\frac{dr}{dt} = -\frac{r}{2}\left(\frac{r^2}{4} - 1 + k\sin\tau\right)$$

$$\frac{r\dot{\phi}}{\epsilon} = \frac{r}{\epsilon}\frac{d\phi}{dt} = -\frac{r}{2}k\cos\tau$$

This of course is an expected result, but is interesting to compare the workload associated with the two solutions. The application of each method was straightforward; however, the two-timing approach was more algebraically rigorous.

4 Nonlinear Analysis

Nonlinear analysis can be used to evaluate the fixed points of the amplitude and phase differential equations in order to quantify the system behavior. The $\dot{r}$ equation has two fixed points at $r = 0$ and $r = 2\sqrt{1 - k\sin\tau}$ if $(1 - k\sin\tau) > 0$. Note that only the positive square root is taken. In that case, the fixed point at $r = 0$ is unstable and all solutions go to $r = 2\sqrt{1 - k\sin\tau}$. Thus, returning to the solution for $x(t)$ from the KBM equations, $x(t) = r(t)\cos[t+\phi(t)]$, the steady-state solution of $x(t)$ can be determined. This is obviously an oscillatory solution, and hence the limit cycle will exist if $(1 - k\sin\tau) > 0$.

$$x(t) = 2\sqrt{1 - k\sin\tau}\cos\left[\left(1 - \frac{\epsilon}{2}k\cos\tau\right)t\right] \tag{23}$$

If $(1 - k\sin\tau) < 0$, there is only one stable fixed point at $r = 0$. So, what conclusion can be drawn from this analysis? If k and τ are chosen such that $r = 0$ is the only fixed point, then the limit cycle will be destroyed and all initial conditions will tend to zero.

4.1 Simulation Results

Several numerical examples are to presented to confirm the nonlinear analytical results above. The true solution modeled with the delay, equation (2), is compared to the solution found using the amplitude and phase ODEs and the predicted steady-state solution from

equation (23). The phase portraits for the DDE and the ODE solutions are also compared. The DDE numerical results were simulated using a fourth-order Runge-Kutta method with initial conditions $\boldsymbol{x}(t-\tau) = \boldsymbol{x}_0$ for $t \in [0, \tau]$, where $\boldsymbol{x} = [x, \dot{x}]^T$.

Figures 1 and 2 show the behavior for $\tau = 0.1$ and $k = 0.1$. For this choice of parameters, $(1 - k \sin \tau) = 0.99 < 1$, and thus, all solutions will approach the limit cycle. This result is confirmed with the numerical simulation. The trajectories in Figure 1 remain close over the time scale of 100 time units. In addition, the shape of the true phase portrait can be closely approximated by the ODE phase portrait.

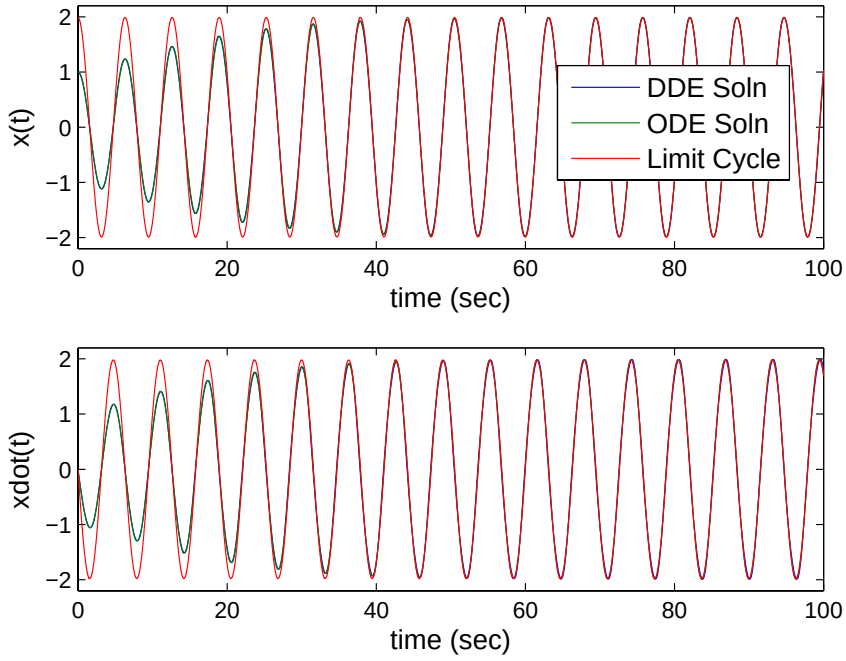

Fig. 1: Comparison of numerical results for the DDE, ODE, and the steady-state solution for k=0.1 and τ=0.1.

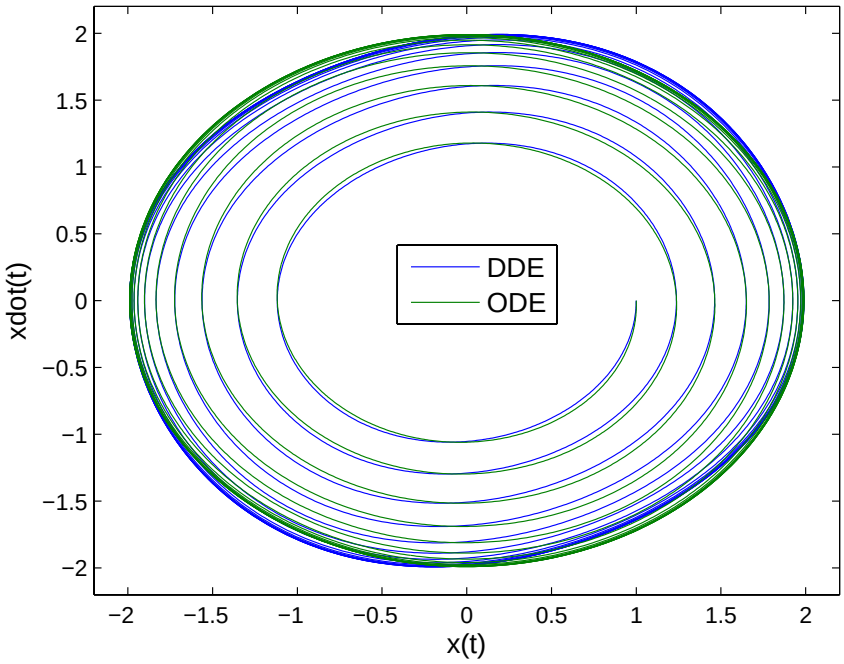

Fig. 2: Comparison of the phase portraits for the DDE and ODE solutions for k=0.1 and τ=0.1.

Figures 3 and 4 show the behavior for $\tau = 0.1$ and $k = 5$, which also predicts a limit cycle. In this case, the steady-state solution correctly predicts the amplitude of the DDE solution; however, the frequency is not closely matched after a short time has elapsed. In addition, the amplitude of the $\dot{x}(t)$ solution is not well-matched to the ODE solution.

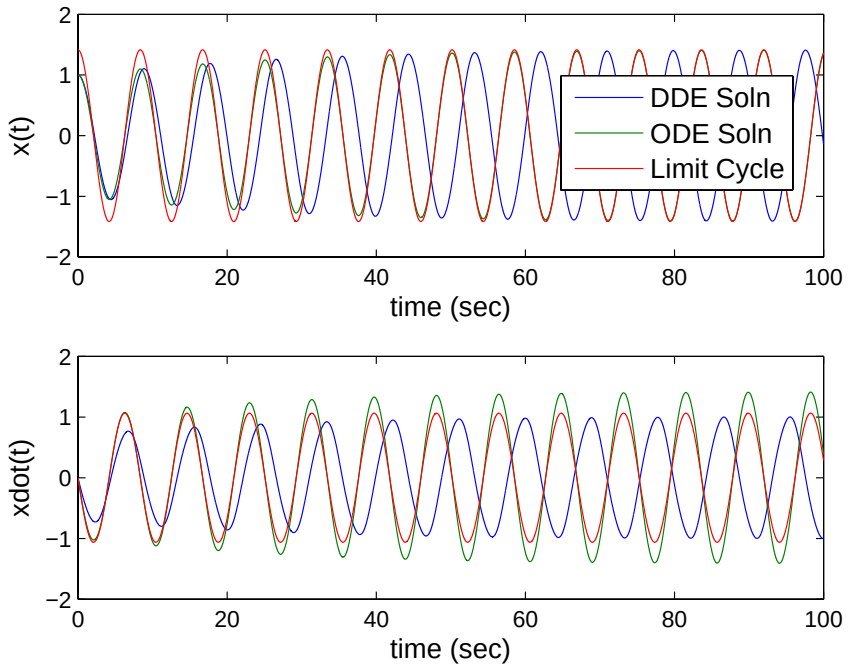

Fig. 3: Comparison of numerical results for the DDE, ODE, and the steady-state solution for k=0.1 and τ=5.

To understand why the $\dot{x}(t)$ solution is less accurate for the second set of parameters, the KBM constraint, $\dot{r}\cos(t+\phi) - r\dot{\phi}\sin(t+\phi)$, was plotted for each of the parameter sets presented. In the formulation of the solutions, this constraint was assumed equal to zero. The constraint evaluated for the first parameter set is much closer to zero than the constraint for the second parameter set.

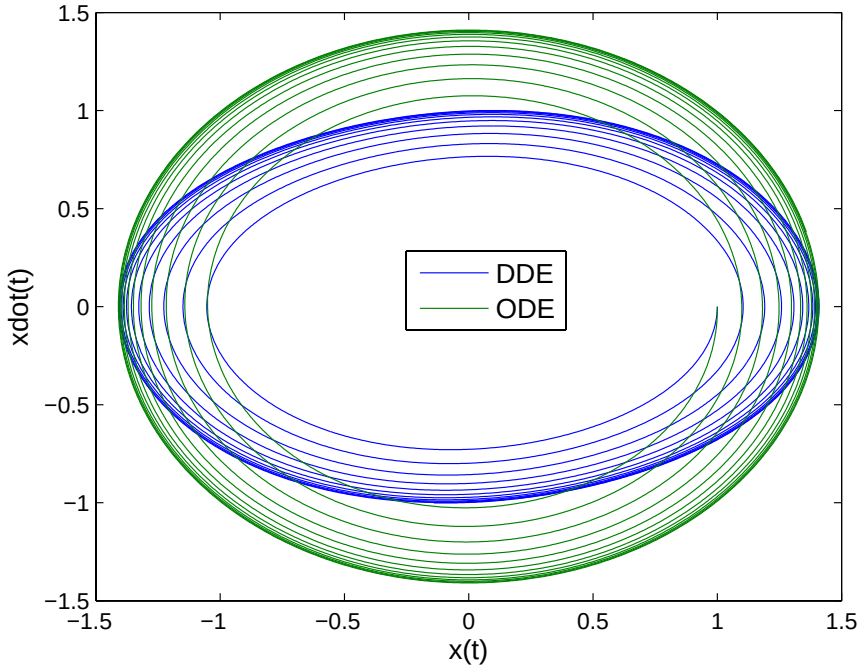

Fig. 4: Comparison of the phase portraits for the DDE and ODE solutions for k=0.1 and τ=5.

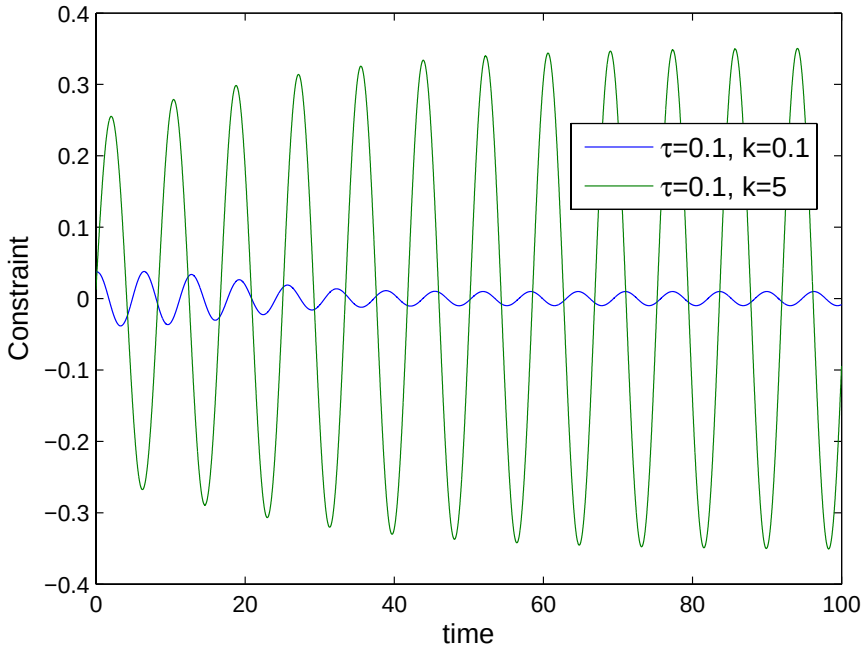

Fig. 5: Comparison of the KBM constraint for (k,τ) = (0.1,0.1) and (0.1,5).

Figures 6 and 7 show the behavior for $\tau = 1$ and $k = 1$, which indicates that the solution should approach the zero solution and limit-cycle behavior will not be observed. In this

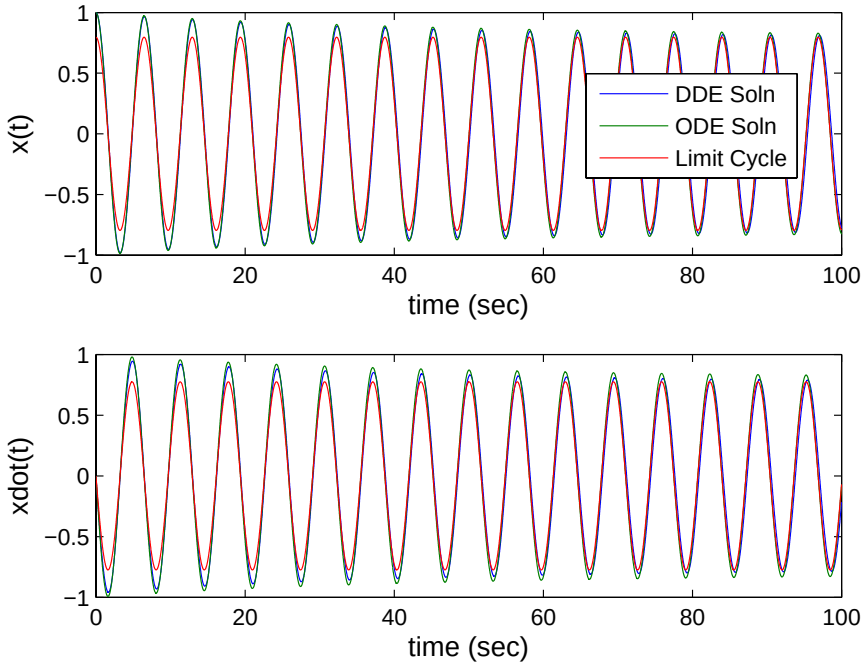

Fig. 6: Comparison of numerical results for the DDE, ODE, and the steady-state solution for k=1 and τ=1.

case, the KBM constraint is close to zero. For this choice of parameters, the states go to zero slowly as seen with the slow decay of the oscillatory behavior and the slow, stable spiral in the phase portrait.

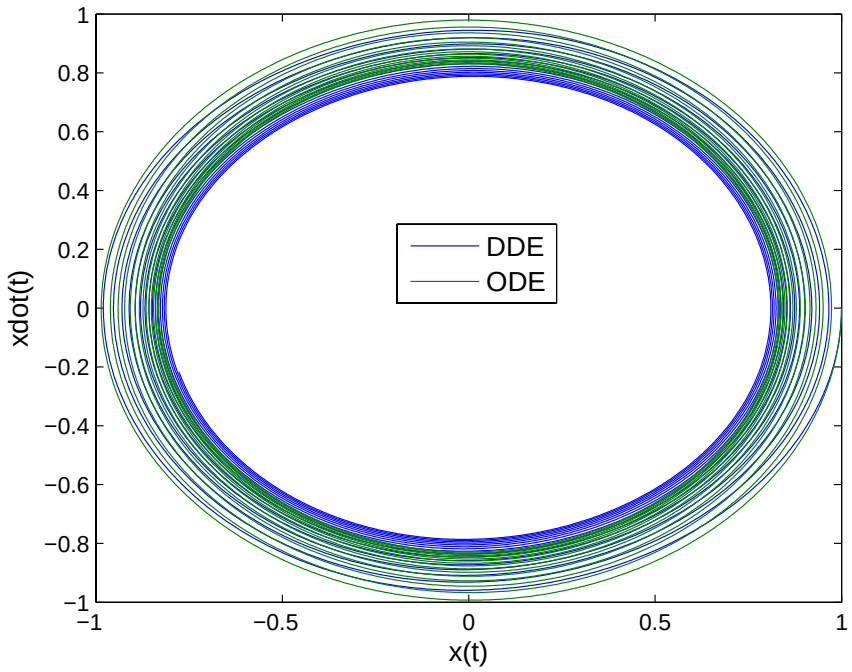

Fig. 7: Comparison of the phase portraits for the DDE and ODE solutions for k=1 and τ=1.

Figures 8 and 9 show the behavior for $\tau = 1$ and $k = 3$. Here, the zero solution is reached within the time scale shown.

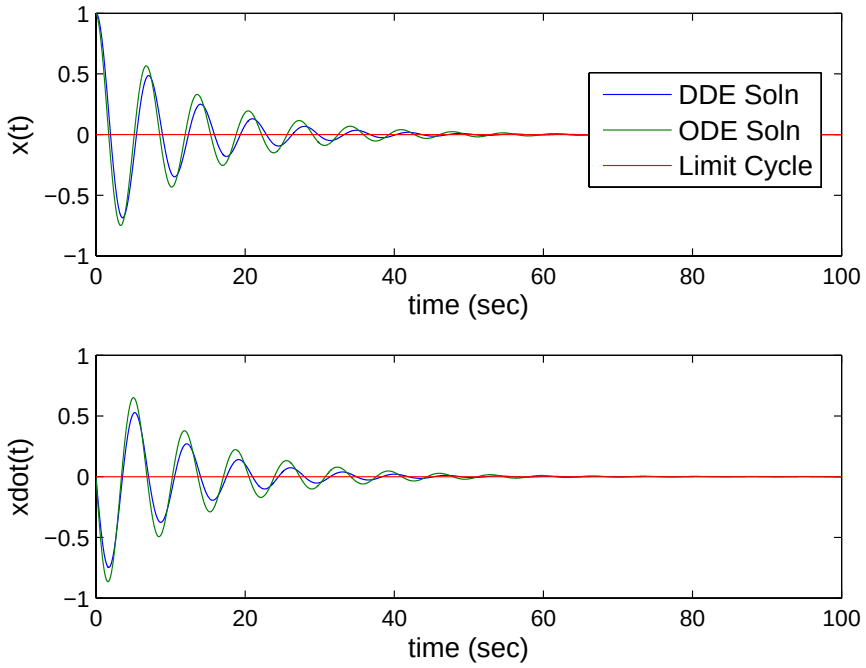

Fig. 8: Comparison of numerical results for the DDE, ODE, and the steady-state solution for k=1 and τ=3.

The numerical results shown correctly predict the presence of the limit cycle. A *supercritical* Hopf bifurcation exists when the value $(1 - k \sin \tau)$ passes through zero. The limit-cycle/non-limit-cycle behavior can be predicted from the stability diagram in the (τ, k) space. The diagram suggests that any parameters chosen from the no-limit-cycle set will drive the system to zero. However, the analysis did not specifically take into account the stability of the original, nonlinear DDE. The trajectories for the parameter choices of (τ, k) = (1,9), (1,10), (1,11) are shown in the following figures, respectively. In Figure 11, the trajectories go to zero as predicted by the amplitude and phase equations. In Figure 12, the

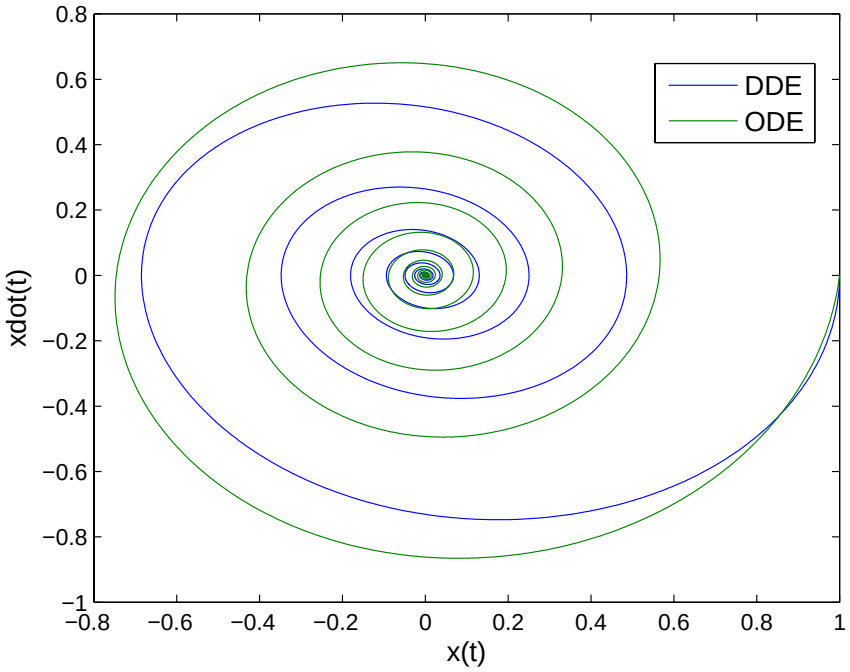

Fig. 9: Comparison of the phase portraits for the DDE and ODE solutions for k=1 and τ=3.

DDE results show that the solution will not move from its initial condition for $\tau = 1$ and $k = 10$ contrary to the prediction from the amplitude and phase equations, and in Figure 13, the DDE results show instabilities. These instabilities are not unexpected because no stability bounds on the parameters in the nonlinear DDE were imposed. Thus, there are sets of the parameters (τ, k) for which the DDE will be unstable. This aspect was missing from Atay's work[2] and should be explored to revise the stability bounds that were presented in Figure 10. Again, the bounds presented in that figure only took into account the behavior from the ODEs that approximated the amplitude and phase of the limit cycle.

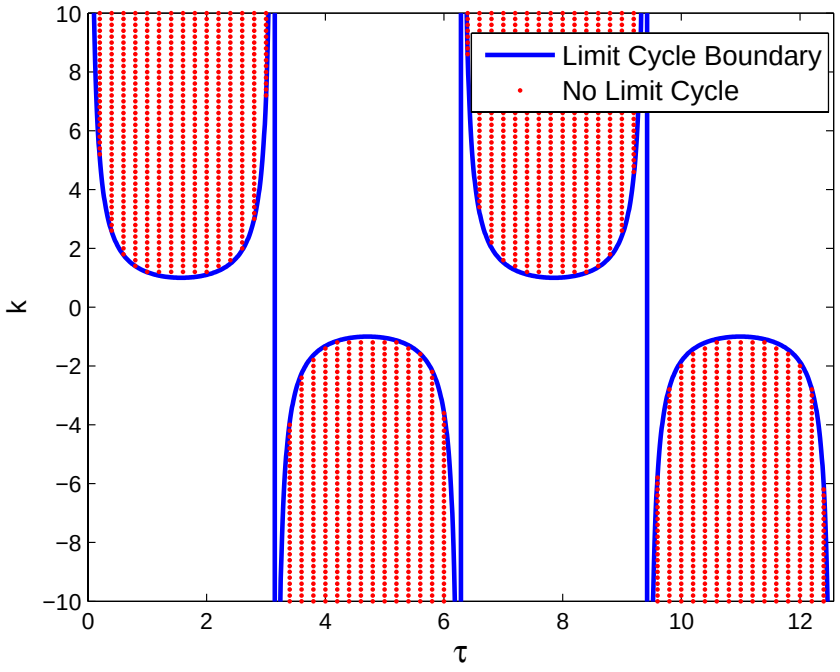

Fig. 10: Limit cycle prediction in the (τ, k) space.

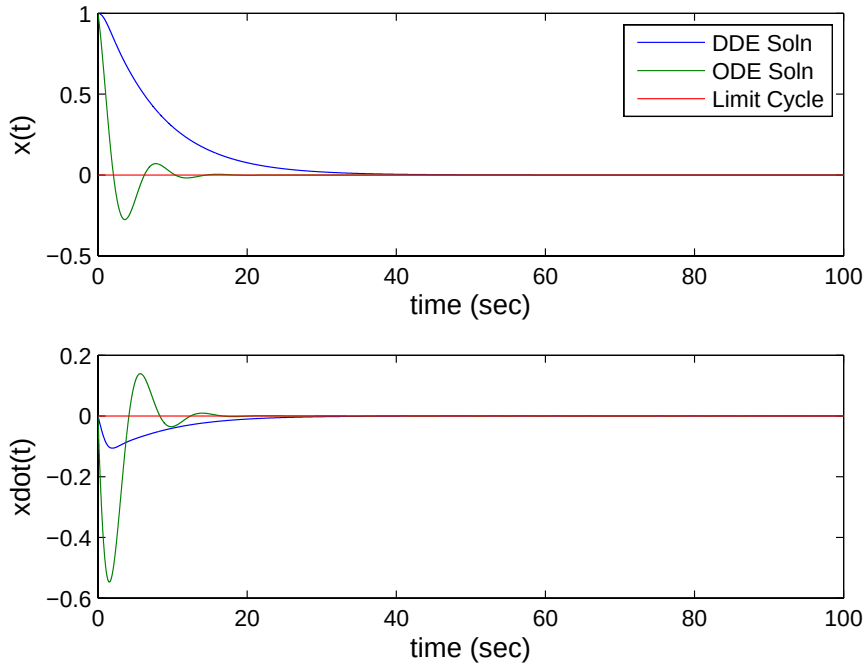

Fig. 11: Limit cycle prediction in the (τ, k) space where $\tau = 1$ and $k = 9$.

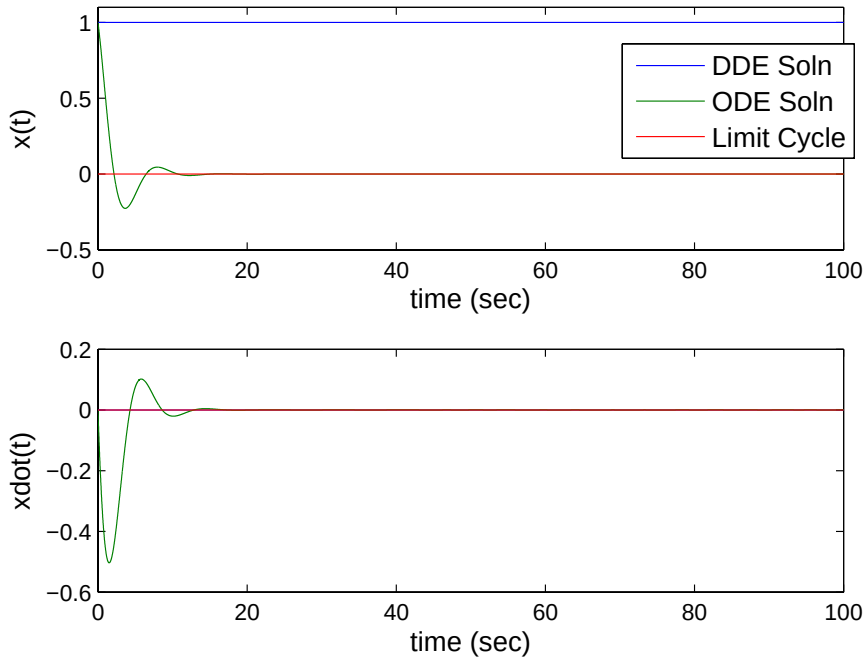

Fig. 12: Limit cycle prediction in the (τ, k) space where $\tau = 1$ and $k = 10$.

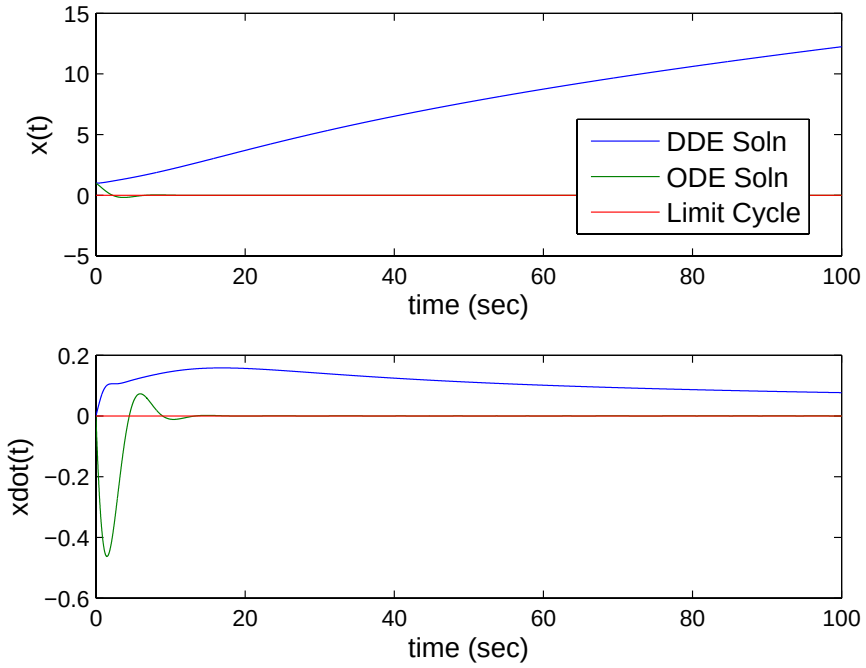

Fig. 13: Limit cycle prediction in the (τ, k) space where $\tau = 1$ and $k = 11$.

4.2 Comparison to Full-State Feedback

Overall, both the averaging and two-timing multiple-scales techniques have been shown to predict the disappearance of limit-cycle behavior for certain choices of feedback position gain and time delay. An interesting result is to compare the delayed feedback to a full-state feedback control of the form $f(t) = \epsilon[k_1 x(t) + k_2 \dot{x}(t)]$. Following the same steps as those presented for either the averaging or the two-timing methods, differential equations for the amplitude and phase can be found.[2]

$$\dot{r} = -\frac{\epsilon r}{2}\left(\frac{r^2}{4} - 1 - k_2\right)$$

$$\dot{\theta} = -\frac{\epsilon}{2}k_1$$

One can see that the position feedback with no delay only impacts the phase, and velocity feedback is necessary to change the amplitude. Hence, the limit cycle cannot be damped using position feedback only without delay.

5 Discussion and Conclusions

This project examined methods to approximate the limit-cycle behavior of the van der Pol oscillator with delayed position feedback, which results in a delay-differential equation (DDE). Due to the nature of the *weakly damped* van der Pol oscillator that exhibits both fast and slow time scales, a multiple-scales perturbation approach was applied to the DDE. Both averaging and two-timing methods were used to derive amplitude and phase equations to describe the limit-cycle behavior; these equations become nonlinear ODEs, and thus, nonlinear analysis can be used to characterize the fixed points and behavior of the ODEs. As

expected, the amplitude and phase equations were identical when derived from the averaging and two-timing methods. From the nonlinear analysis, a *supercritical* Hopf bifurcation occurs, and the limit-cycle can be eliminated by appropriating choosing the position-feedback gain and time delay.

Following the investigation on the nonlinear DDE behavior, several additional research areas are suggested:

1. Further analysis on the stable regions of the original DDE should be merged with the stability regions where the limit-cycle is eliminated.

2. Wang and Hu[9] indicate some ambiguities in the stability analysis of periodic, nonlinear DDEs when a higher-order approximation of the method of multiple scales is used. This project used a second-order approximation; however, the same stability results will not be derived when a third-order approximation is investigated. The van der Pol oscillator with delayed position feedback should be explored using the higher-order approximation, and results should be compared to the Wang and Hu results for the duffing oscillator.

3. Numerical results for the nonlinear DDE should also be explored using a numerical toolbox, such as DDE-BIFTOOL. It would be interesting to compare the bifurcation results using a continuation method to the analytical results derived here. Whereas this tool was examined for its applicability to this project, more time must be spent to understand the numerical methods that DDE-BIFTOOL applies.

A Derivatives Used in the Two-Timing Method

The solution to the equation $D_0^2 x_0 + x_0 = 0$ is $x_0(T_0, T_1) = A(T_1)e^{iT_0} + \bar{A}(T_1)e^{-iT_0}$. The following expressions and derivatives are needed in the two-timing approach.

$$D_0 x_0(T_0, T_1) = iA(T_1)e^{iT_0} - i\bar{A}(T_1)e^{-iT_0} = iA(T_1)e^{iT_0} + cc \tag{24}$$

$$D_1 D_0 x_0(T_0, T_1) = iA'(T_1)e^{iT_0} - i\bar{A}'(T_1)e^{-iT_0} = iA'(T_1)e^{iT_0} + cc \tag{25}$$

$$\begin{aligned}
[x_0(T_0, T_1)]^2 &= \left[A(T_1)e^{iT_0} + \bar{A}(T_1)e^{iT_0}\right]^2 \\
&= A^2(T_1)e^{i2T_0} + 2A(T_1)\bar{A}(T_1) + \bar{A}(T_1)^2 e^{-i2T_0} \\
&= A^2(T_1)(T_1)e^{i2T_0} + 2A(T_1)\bar{A}(T_1) + cc
\end{aligned} \tag{26}$$

$$\begin{aligned}
[x_0(T_0, T_1)]^2 D_0 x_0(T_0, T_1) &= \left[A^2(T_1)e^{i2T_0} + 2A(T_1)\bar{A}(T_1) + \bar{A}(T_1)^2 e^{-i2T_0}\right](iA(T_1)e^{iT_0} - i\bar{A}(T_1)e^{-iT_0}) \\
&= iA^3(T_1)e^{i3T_0} + iA^2(T_1)\bar{A}(T_1)e^{iT_0} + cc
\end{aligned} \tag{27}$$

References

[1] Strogatz, S. H., *Nonlinear Dynamics and Chaos*, Perseus Books Publishing, Cambridge, MA, 1994, Chapter 7.

[2] Atay, F. M., "Van der Pol's Oscillator under Delayed Feedback," *Journal of Sound and Vibration*, Vol. 218, 1998, pp. 333–339.

[3] Maccari, A., "The Response of a Parametrically Excited van der Pol Oscillator to a Time Delay State Feedback," *Journal of Nonlinear Dynamics*, Vol. 26, 2001, pp. 105–119.

[4] Hu, H., Dowell, E. H., and Virgin, L. N., "Resonances of a Harmonically Forced Duffing Oscillator with Time Delay State Feedback," *Journal of Nonlinear Dynamics*, Vol. 15, 1998, pp. 311–327.

[5] Hale, J., *Theory of Function Differential Equations*, Springer-Verlag, New York, NY, 1977.

[6] Driver, R. D., *Ordinary and Delay Differential Equations*, Springer-Verlag, New York, NY, 1977, Chapter 5.

[7] Kalmàr-Nàgy, T., *Delay Differential Models of Cutting Tool Dynamics with Nonlinear and Mode-Coupling Effects*, Ph.D. thesis, Cornell University, Ithaca, New York, 2002.

[8] Nayfeh, A. H., *Introduction of Perturbation Techniques*, John Wiley and Sons, Inc., New York, NY, 1981.

[9] Wang, H. and Hu, H., "Remarks on the Perturbation Methods in Solving the Second-Order Delay Differential Equations," *Journal of Nonlinear Dynamics*, Vol. 33, 2003, pp. 379–398.